On the kinematics of water waves through a porous plate

Qunbin Chen[1], Junnan Cui[1], Qiang Liu[1], Xingya Feng[1,*], Yuming Liu[2], Song An[1], and Jian-Fei Chen[1]

[1] Department of Ocean Science and Engineering, Southern University of Science and Technology, Shenzhen, China.
[2] Department of Mechanical Engineering, Massachusetts Institute of Technology, Cambridge, USA
E-mail: fengxy@sustech.edu.cn

Highlights

- We examine two quadratic pressure drop conditions in the model of wave passing through a porous plate.
- Velocity fields near the porous plate were measured by a particle image velocimetry (PIV) in the tank tests.
- Flow patterns display a significant distinction on the windward and leeward sides of the porous plate.

1 Introduction

Porous structures have been widely used in ocean engineering, such as perforated breakwaters, fish farms, and tuned damper/stabilizer. Flow separation is the primary physical feature when waves pass porous structures. As a result, wave energy can be dissipated by the formation of vortices, jets and eddy zones. Therefore, porous structures can effectively reduce wave reflections and transmissions, as well as wave forces acting on the structures.

To calculate hydrodynamic characteristics of wave interactions with porous structures in the framework of potential flow model, the key issue is to ascertain proper boundary conditions on porous boundaries. The issue turns to determine the relationship between the pressure drop through a porous plate and the local velocity. Two types of porous boundary conditions are commonly used. The first one is the linear pressure drop condition (LPDC), which established a linear relationship between pressure drop and the velocity on the porous boundary. It was initially proposed by Sollitt and Cross (1972)[1] and further developed by Yu (1995)[2]. LPDC is easy to implement in theoretical models. However, it needs to correct empirical coefficients on the linearized resistance coefficient C_r and the added-mass coefficient C_m according to the measurement at different experimental conditions. The second one is the quadratic pressure drop condition (QPDC), in which pressure loss is proportional to the square of the normal velocity on porous boundaries. Mei et al. (1974)[3] first proposed a QPDC on long waves, which also included a linear term related to inertia effect. Molin (1993)[4] presented another forms of QPDC. Compared to the LPDC, coefficients in the QPDC are related to geometric configuration, which are not required to calibrate by physical experiments. Models using the QPDC have been shown to be more effective than that using LPDC in predicting wave reflection/transmission coefficients[5] and damping coefficients[6]. However, few works investigate the local kinematics close to the porous plate, such as velocity field and pressure distribution. In the present work, we employ two QPDCs in the theoretical model, and examine the performance for the two QPDCs[3, 4] in predicting the local velocity and pressure around a porous plate. Experiments were also carried out to obtain velocity field and pressure distribution near the porous plate, where velocities were measured by using the method of particle image velocimetry (PIV).

2 Theoretical formulation

We consider surface gravity waves passing through a vertical porous plate, which consists of a finite number of thin plates. A Cartesian coordinate system (x, z) is defined with origin O at the intersection of the porous plate and the mean water surface, and the direction of incident waves points to the positive x-axis, as shown in Fig. 1. Assume the fluid is ideal fluid, i.e., incompressible, inviscid and the flow is irrotational. We further assume the incident wave height H is sufficiently small such that a linearized free surface condition is considered. The fluid motion can thus be described by a velocity potential Φ, which satisfies the Laplace equation within the fluid region, the linearized free surface condition, and no flow condition on the flat bottom. Within the framework of the linear potential theory, the velocity potential $\Phi(x, z, t)$ can be written as

$$\Phi(x,z,t)=\mathrm{Re}\left\{-\frac{\mathrm{i}HgN_0}{2\omega\cosh kh}\phi(x,z)\mathrm{e}^{-\mathrm{i}\omega t}\right\} \tag{1}$$

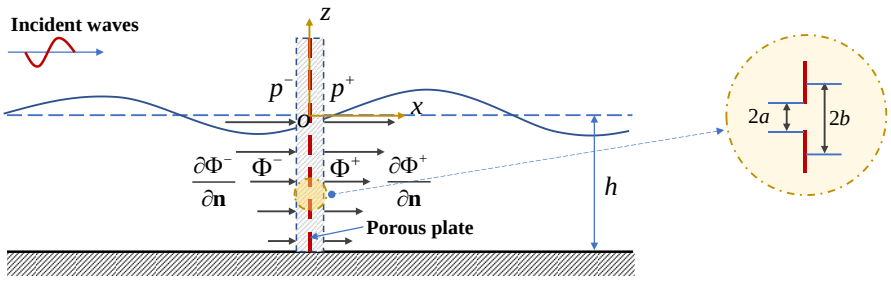

Fig. 1 Schematic diagram of surface gravity wave interaction with a porous plate

where $\mathrm{Re}\{\cdot\}$ denotes the real part of the argument, $\mathrm{i}=\sqrt{-1}$, and g is the acceleration due to gravity; ω and k represent radian frequency and wavenumber, respectively.

On the windward side of the porous plate $\phi(x, z)$ can be expressed as

$$\phi_-(x,z)=\left(\mathrm{e}^{\mathrm{i}kx}+R\mathrm{e}^{-\mathrm{i}kx}\right)\psi_0(z)+\sum_{n=1}^{\infty}A_n\mathrm{e}^{k_nx}\psi_n(z);\quad x<0, \tag{2}$$

and on the leeward side of the porous plate $\phi(x, z)$ can be written by

$$\phi_+(x,z)=T\mathrm{e}^{\mathrm{i}kx}\psi_0(z)+\sum_{n=1}^{\infty}B_n\mathrm{e}^{-k_nx}\psi_n(z);\quad x>0, \tag{3}$$

where R and T are complex constants, and their modulus denote reflection and transmission coefficients; A_n and B_n represent the coefficients for the n-th evanescent mode;

$$\psi_n(z)=N_n^{-1}\cos k_n(z+h),\quad N_n^2=\frac{1}{2}\left(1+\frac{\sin 2k_nh}{2k_nh}\right),\quad n=0,1,2,\cdots;$$

with

$$\omega^2=gk\tanh kh;\quad \text{and}\quad \omega^2+gk_n\tan k_nh=0,\quad n=1,2,\cdots.$$

On the boundary of the porous plate, continuity of the normal velocity requires that

$$\frac{\partial\Phi_-}{\partial x}=\frac{\partial\Phi_+}{\partial x},\quad \text{for } x=0 \text{ and } -h\le z\le 0. \tag{4}$$

A pressure jump condition on the porous boundary is considered. In this work, we use two QPDCs. One was proposed by Mei et al. (1974)[3]. In the present problem, it can be written as

$$\Delta p=p_--p_+=\rho\left(\frac{F}{2}\frac{\partial\Phi_+}{\partial x}\left|\frac{\partial\Phi_+}{\partial x}\right|+L\frac{\partial^2\Phi_+}{\partial t\partial x}\right),\quad \text{for } x=0 \text{ and } -h\le z\le 0. \tag{5}$$

Here ρ denotes the fluid density; the head loss coefficient F and the effective orifice length L are calculated by

$$F=\left[\frac{1}{\tau\left(0.6+0.4\tau^2\right)}-1\right]^2,\quad \text{and}\quad L=\frac{2b}{\pi}\ln\frac{1}{2}\left(\tan\frac{\pi}{4}\tau+\cot\frac{\pi}{4}\tau\right),$$

where the porosity is $\tau=a/b$ with $2a$ and $2b$ being the width of the opening and two adjacent thin plates, respectively.

The other QPDC used in this work is based on Molin (1993)[4], i.e.,

$$\Delta p=\frac{1-\tau}{2\mu\tau^2}\rho\frac{\partial\Phi_+}{\partial x}\left|\frac{\partial\Phi_+}{\partial x}\right|,\quad \text{for } x=0 \text{ and } -h\le z\le 0. \tag{6}$$

The discharge coefficient μ was taken equal to 0.5 as suggested in Molin and Remy (2013)[6].

3 Experimental set-up

The experiments were carried out in the wave flume at Southern University of Science and Technology. The wave flume is 20 m long, 1.0 m wide and 1.2 m deep; the water depth was set as 0.5 m. A piston-type wavemaker was used to generate incident waves. A sloping beach was equipped at the other end to prevent reflection of waves. A porous plate with a 2 cm thickness was placed at 7.5 m away from the wavemaker and spanned the width of the wave flume. The plate has 56 circular openings with a 25.2 mm diameter for each hole, which results in a plate porosity of 0.2.

A PIV technique was employed to measure velocity fields around the porous plate. The PIV measurements have a field of view (FOV) of 0.7 m × 0.3 m in horizontal and vertical directions, respectively. The porous plate was located in the horizontal center of the FOV, and the free surface was located at the top of the FOV. Eight pressure sensors were used to measure pressure variations along the water depth. On the windward side x = -0.2 m, there are four pressure sensors located at z = -0.03 m, -0.08 m, -0.23 m and -0.38 m; the other four pressure sensors were located on the leeward side x = 0.2 m with the same z values as the windward side.

4 Results, discussion and conclusions

Fig. 2(a)-(c) compare horizontal velocity profiles between the theoretical results and the experimental data on the windward side of the porous plate, i.e., x = -0.3 m, and the leeward side x = +0.3 m with the plate porosity τ = 0.2 for kh = 1.44, 2.91 and 5.15. They correspond to wave frequencies of 0.8 Hz, 1.2 Hz and 1.6 Hz, respectively. Here the incident wave height is fixed at 0.02 m for the three wave frequencies. It can be found that the value of horizontal velocity profiles based on the QPDC with the model of Molin (1993)[4] is larger than that of the QPDC with Mei et al. (1974)[3]. But the difference between the two QPDCs is small, which means the dominant contribution on the porous boundary is drag effects at the present wave conditions. Compared to the experimental data, it can be found that the theoretical results of the horizontal velocity profiles agree well with the experimental data for kh = 1.44, 2.91 and 5.15. At the same wave conditions, Fig. 3(a)-(c) display dynamic pressure variations along water depth at x = -0.2 m and x = +0.2 m. Overall, the theoretical results are consistent with the experimental data, and the value of dynamic pressure on the windward side of the porous plate is larger than that on the leeward side.

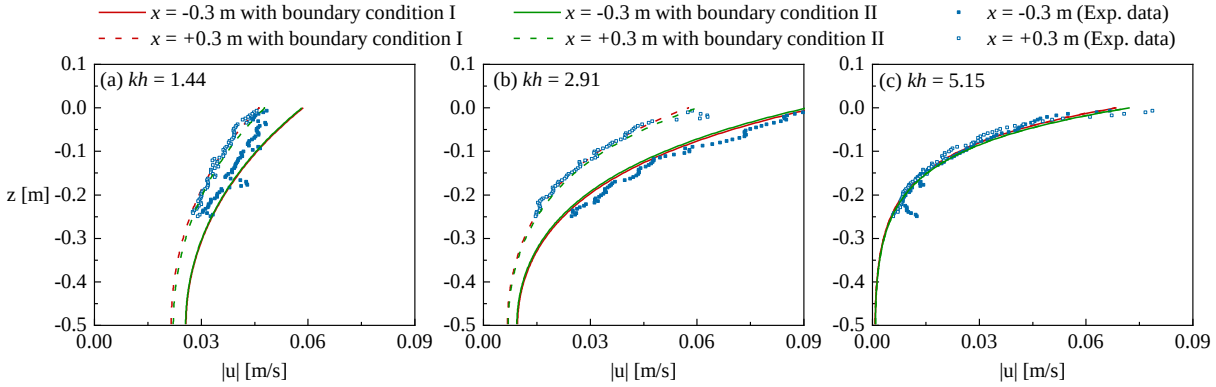

Fig. 2 Comparison of horizental velocity profiles between theoretical results (solid and dashed lines) and experimental data (scatters) at x = -0.3 m and x = +0.3 m with porosity τ = 0.2 for (a) kh = 1.44, (b) kh = 2.91 and (c) kh = 5.15, where two pressure drop conditons were used in the theoretical model: boundary conditon I for Mei et al. (1974)[3], boundary conditon II for Molin (1993)[4]

We further examine horizontal velocity variations along x-axis at z = -0.05 m, -0.1 m and -0.2 m for kh = 5.15, as shown in Fig. 4. The experimental data were measured within 0.7 m in horizontal range due to the limitation of FOV in PIV. Hence, we only display the short wave case, i.e., kh = 5.15. The theoretical results are obtained based on the QPCD with Mei et al. (1974)[3]. It is interesting to find that flow patterns on the windward side of the porous plate is considerably different from that on the leeward side. The reason for this might be due to the superposition of incident waves and reflection waves on the windward side, which results in the appearance of partial standing waves. On the leeward side

there only exists transmission waves. That causes the flow patterns on either side of the porous plate different. More detailed discussion and interpretation of the results will be presented at the workshop, especially for the local oscillation of velocity fields near the porous plate.

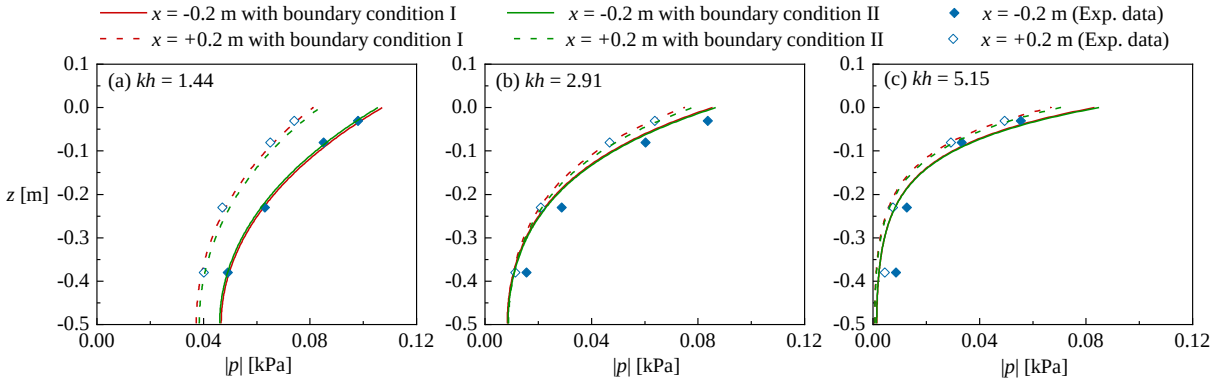

Fig. 3 Comparison of dynamic pressure variations along water depth between theoretical results (solid and dashed lines) and experimental data (scatters) at x = -0.2 m and x = +0.2 m with porosity $\tau = 0.2$ for (a) kh = 1.44, (b) kh = 2.91 and (c) kh = 5.15

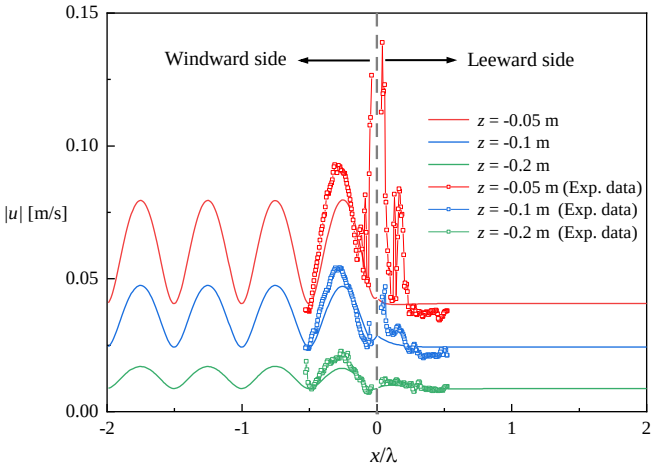

Fig. 4 Comparison of horizontal velocity variations along the x-axis between theory results and experimental data for kh = 5.15

Acknowledgements

The work has been partially supported by the Natural Science Foundation of China for Young Scholars (12202175). The authors would also like to acknowledge the support by Centers for Mechanical Engineering Research and Education at MIT and SUSTech.

References

[1] Sollitt CK, Cross RH. Wave transmission through permeable breakwaters. In: *13th Int. Conf. on Coast. Eng.*, July 10-14, 1972, Vancouver, Canada.

[2] Yu XP. Diffraction of water waves by porous breakwaters. *J. Waterw. Port Coast. Ocean Eng.*, 1995, 121:275-282.

[3] Mei CC, Liu PL, Ippen AT. Quadratic loss and scattering of long waves. *J. Waterw. Port Coast. Ocean Eng.*, 1974, 100:217-239.

[4] Molin B. A potential flow model for the drag of shrouded cylinders. *J. Fluids Struct.*, 1993, 7:29-38.

[5] Bennett GS, McIver P, Smallman JV. A mathematical model of a slotted wavescreen breakwater. *Coast. Eng.*, 1992, 18:231-249.

[6] Molin B, Remy F. Experimental and numerical study of the sloshing motion in a rectangular tank with a perforated screen. *J. Fluids Struct.*, 2013, 43:463-480.